

Nuisances via Negativa: Adjusting for Spurious Correlations via Data Augmentation

Aahlad Puli¹ Nitish Joshi¹ He He^{1,2} Rajesh Ranganath^{1,2,3}

¹Department of Computer Science, New York University

²Center for Data Science, New York University

³Department of Population Health, Langone Health, New York University

Abstract

In prediction tasks, there exist features that are related to the label in the same way across different settings for that task; these are semantic features or *semantics*. Features with varying relationships to the label are *nuisances*. For example, in detecting cows from natural images, the shape of the head is a semantic but because images of cows often have grass backgrounds but not always, the background is a nuisance. Relationships between a nuisance and the label are unstable across settings and, consequently, models that exploit nuisance-label relationships face performance degradation when these relationships change. Direct knowledge of a nuisance helps build models that are robust to such changes, but requires extra annotations beyond labels and covariates. In this paper, we develop an alternative way to produce robust models by data augmentation. These data augmentations corrupt semantic information to produce models that identify and adjust for where nuisances drive predictions. We study semantic corruptions in powering different spurious-correlation avoiding methods on multiple out-of distribution (OOD) tasks like classifying waterbirds, natural language inference (NLI), and detecting cardiomegaly in chest X-rays.

1 Introduction

Relationships between the label and the covariates can change across data collected at different places and times. For example, in classifying animals, data collected in natural habitats have cows appear on grasslands, while penguins appear on backgrounds of snow; these animal-background relationships do not hold outside natural habitats [1, 2]. Some features, like an animal’s shape, are predictive of the label across all settings for a task; these are semantic features, or semantics in short. Other features with varying relationships with the label, like the background, are nuisances. Even with semantics present, models trained via empirical risk minimization (ERM) can predict using nuisances and thus fail to generalize [3].

Models that rely only on the semantic features perform well even when the nuisance-label relationship changes, unlike models that rely on nuisances. Many methods exist to build models robust to changing nuisance-label relationships [4, 5, 6, 7, 8]; we call these spurious-correlation avoiding methods (SCAMs). These methods broadly fall into two classes: 1) methods that assume access to nuisances, like Nuisance-Randomized Distillation (NURD) [7], debiased focus loss (DFL), product of experts (POE) [4], and 2) methods that rely on assumptions about ERM-trained models relying on nuisances, like Just Train Twice (JTT) [6]. We point out a commonality between the two classes of methods: a model that predicts the label from the nuisance called a *biased model*. Biased models play a role in building robust predictive models by detecting when the nuisance can influence predictions. These models are built using extra nuisance annotations or assumptions about ERM-trained models relying on nuisances.

Instead, imagine using data augmentation to corrupt the semantics in the covariates — if the resulting semantic-corrupted input can still predict the label, the prediction must rely on nuisances, thereby providing a window into nuisances that help build a biased model. Designing a data augmentation that corrupts

¹Corresponding email: aahlad@nyu.edu.

semantics is easy. For example, replacing the covariates with random noise would fully corrupt the semantics. However, such corruptions do not leave nuisances behind. Corruptions that retain some nuisances are better for building biased models. Though, corruptions can be used in a manner that even if all the nuisances are destroyed the performance is no worse than the underlying SCAM without the semantic corruption. We use semantic knowledge to develop corruptions for object recognition and NLI that retain some features, and use these corruptions to build biased models for SCAMs.

The first corruption we design is for global semantics. Formally, global semantics are position-dependent functions of the subsets of the covariates (e.g patches in images, or words in sentences). For example, in recognizing cows, the shape of the animal structures the distant patches where the cow’s eyes, tail, and hooves appear. We corrupt global semantics by randomizing subset-position via patch randomization (PATCH-RAND) for images and n-gram randomization (NGRAM-RAND) for NLI.

The second corruption is designed for semantics that require certain parts of the input. In NLI, the premise sets up the context for detecting entailment. Without the premise, entailment cannot be determined by semantics. Masking parts of the covariates corrupts location-based semantics for object recognition via region-of-interest masking (ROI-MASK) and for the semantic context in NLI via premise masking (PREM-MASK).

The next two corruptions focus on characterizing semantics in terms of the associated frequencies and brightness. For example, in detecting cardiomegaly in chest X-rays, semantic features like the heart are low-frequency features with high pixel-intensity; see fig. 2. We develop corruptions for such semantics with frequency filtering (FREQ-FILTER) and intensity filtering (INT-FILTER).

We demonstrate the value of semantic corruption by using it to power a variety of SCAMs: NURD [7], DFL, POE [4], and JTT [6]. We run these methods by building biased models using nuisances produced by semantic corruption. These methods with semantic corruptions outperform ERM on OOD generalization tasks like waterbirds [9], cardiomegaly detection from chest X-rays, and NLI. The performance of NURD, DFL, POE run with semantic corruption is similar to what the methods achieve with extra observed nuisance variables. JTT with semantic corruptions outperforms vanilla JTT.

2 Spurious correlation avoiding methods

A spurious correlation is a relationship between the covariates and the label that changes across settings like time and location [3]. Models that exploit a spurious correlation can perform poorly outside the training distribution. We focus on the class of methods that correct models using knowledge of nuisances or where they might appear [4, 6, 7]; we call these **spurious-correlation avoiding methods (SCAMs)**. With label y , a vector of nuisances z , and covariates x , the goal is to predict well on data regardless of the nuisance-label relationship. Next, we establish that the central part of several SCAMs is a model that predicts the label using nuisances, which we call the biased model. Let p_{tr} and p_{te} be the training and test distributions respectively, and let $a \perp\!\!\!\perp b$ denote that the random variables a, b are independent.

NURD. In tackling spurious correlations, Puli et al. [7] identify a conditional that has performance guarantees on test distribution p_{te} with an unknown nuisance-label relationship. They develop NURD to learn the conditional using data from $p_{tr} \neq p_{te}$. NURD uses 1) the nuisance-randomized distribution, $p_{\perp}(y, z, x) = p(y)p_{\perp}(z)p(x | y, z)$, where $z \perp\!\!\!\perp_{p_{\perp}} y$, and 2) an uncorrelating representation $r(x)$ for which $z \perp\!\!\!\perp_{p_{\perp}} y | r(x)$. In p_{\perp} , the nuisance alone cannot predict the label; this sidesteps features that depend only on the nuisance. Next, features that are mixed functions of the label and the nuisance (e.g. $x_1 = y + z$) can also be spurious. Uncorrelating $r(x)$ avoid such features. With these insights, NURD builds models of the form $p_{\perp}(y | r(x))$ that are most informative of the label. We work with reweighting-NURD, which estimates p_{\perp} by weighting samples as $p(y)/p_{tr}(y | z)p_{tr}(y, z, x)$. See appendix A for more details.

End-to-end bias mitigation. Mahabadi et al. [4] consider two methods to train a biased model and a base predictive model jointly to make the base model predict without relying on the biases. The methods use and fine-tune a BERT model [10] and do not propagate the gradients of the biased model to update the

Table 1: Summary of NURD, JTT, POE, and DFL. Each method approximates the biased model: $p_{tr}(\mathbf{y} | \mathbf{z})$. This table describes the different biased models, their names, how they are built. We build biased models as $p_{tr}(\mathbf{y} | T(\mathbf{x}))$ where $T(\mathbf{x})$ is a semantic corruption.

Method	Name	What the biased model is	Assumptions
JTT	Identification model	$p_{tr}(\mathbf{y} \mathbf{x})$ learned via ERM	ERM builds biased models.
POE/DFL	Biased model	$p_{tr}(\mathbf{y} \mathbf{z})$ learned via ERM	\mathbf{z} from domain-knowledge.
NURD	Weight model	$p_{tr}(\mathbf{y} \mathbf{z})$ learned via ERM	\mathbf{z} from domain-knowledge.

common parameters (token embeddings in this case). They propose 1) POE, where the \log of the product of the predicted probabilities of the two models is used to compute the classification loss and 2) DFL, where the biased model is used to weight the cross-entropy loss for the base model. For both methods, Mahabadi et al. [4] build a biased model as $p_{tr}(\mathbf{y} | \mathbf{z})$. The intuition is that the base model focuses on classifying samples that the biased model misclassifies.

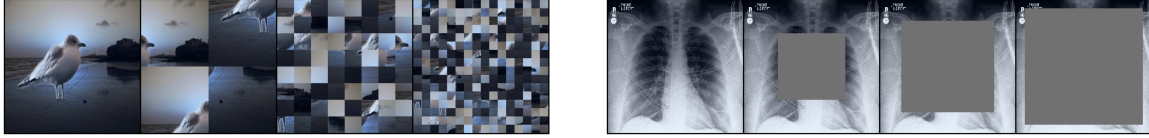
Just Train Twice JTT. With JTT, Liu et al. [6] aim to build models robust to group shift, where the relative mass of a fixed set of disjoint groups of the data changes between training and test times. The groups here are subsets of the data defined by a pair of values of discrete label and nuisance values. While they work without relying on training group annotations, i.e. without nuisances, JTT assumes ERM’s misclassifications are because of a reliance on the nuisance. JTT first builds an “identification” model via ERM to isolate samples that are misclassified. Then, JTT trains a model via ERM on data with the loss for the misclassified samples upweighted (by constant λ). The number of epochs to train the identification model and the upweighting constant are hyperparameters that require tuning using group annotations [6].

The commonality of a biased model. The central part between NURD, DFL, POE, and JTT is a model that predicts the label using nuisances, like $p_{tr}(\mathbf{y} | \mathbf{z})$, which we call the biased model as in He et al. [8]. The predictive models in each SCAM are guided to not depend on nuisances used by the biased model. While SCAMS reduce dependence on nuisances, they build biased models using additional nuisance annotations or require assumptions that ERM-trained models predict using the nuisance. In the next section, we describe an alternative: corrupt semantic information with data augmentations to construct nuisances that can be used in a biased model.

3 Robustness via Semantic Corruptions

We define a data augmentation as a transformation of the covariates with random noise δ : $T(\mathbf{x}, \delta)$. Formally, an ideal semantic corruption is a data augmentation or transformation such that the label does not depend on the transformation given the nuisance $\mathbf{y} \perp\!\!\!\perp T(\mathbf{x}, \delta) | \mathbf{z}$ and that the transformation is not independent of the nuisance $T(\mathbf{x}, \delta) \not\perp\!\!\!\perp \mathbf{z}$. The first condition ensures that the biased model built from the semantic corruption only predicts the label because of the nuisance. The second condition ensures the semantic corruption depends on the nuisance.

These two conditions are in tension in designing a semantic corruption. The former wants to destroy everything about the label unrelated to the nuisance, while the latter wants to retain everything about the nuisance. This tension is mitigated by the fact that for many SCAMS even if all the nuisances are destroyed the performance is no worse than the underlying SCAM without the semantic corruption. For example, NURD without an explicitly observed nuisance reverts to ERM and NURD with a corruption that is pure noise also reverts to ERM. Focusing on two popular OOD tasks, object recognition and NLI, we use only semantic knowledge to build corruptions that retain some features. Biased models built on such corruptions will depend on any retained nuisances; more retained nuisances mean better biased models.



(a) PATCH-RAND to corrupt global semantics in Waterbirds. The original is the left most, followed by PATCH-RANDS with sizes 112, 28, 14. At sizes less than 28, shape is hard to make out.

(b) Masking to corrupt semantics in chest X-rays. The original is the left most, followed by ROI-MASK of size 112, 154, 196. At sizes more than 154, the heart is blocked out.

Figure 1: Semantic corruptions of Waterbirds via PATCH-RAND and chest X-rays via ROI-MASK.

3.1 Semantic corruptions via permutations

We first build corruptions when semantics appear as global structure. We give an intuitive example for such global semantics. Consider the waterbirds dataset from Sagawa et al. [9] with waterbirds and landbirds appearing predominantly on backgrounds with water and land respectively. Semantic features like the wing shape and the presence of webbed feet are corrupted by randomly permuting small patches. See fig. 1a. Formally, given subsets of the covariates $\mathbf{x}_1, \dots, \mathbf{x}_k$ extracted in an order, global semantics $s(\mathbf{x}_1, \dots, \mathbf{x}_k)$ change with the order of extraction: for permutations Π

$$\exists \pi \in \Pi \quad s(\mathbf{x}_1, \dots, \mathbf{x}_k) \neq s(\mathbf{x}_{\pi(1)}, \dots, \mathbf{x}_{\pi(k)}),$$

We give a demonstrative example of a semantic corruption with global semantics. Consider a family of distributions $\mathcal{F} = \{p_D\}_{D \in \mathbb{R}}$ with changing nuisance-label relationships. With \mathcal{U} as the uniform distribution over $\{1, 2, 3\}$, and \mathcal{N} as the normal distribution, samples from $p_D(\mathbf{y}, \mathbf{z}, \mathbf{x})$ come as $\mathbf{y} \sim \mathcal{U}$, $\mathbf{z} \sim \mathcal{N}(D\mathbf{y}, 1)$, and \mathbf{x} selects a configuration of \mathbf{x}

$$\begin{aligned} \mathbf{y} = 1 &\implies \mathbf{x} = [-\mathbf{z}, \mathbf{z}, \mathbf{z}], \\ \mathbf{y} = 2 &\implies \mathbf{x} = [\mathbf{z}, -\mathbf{z}, \mathbf{z}], \\ \mathbf{y} = 3 &\implies \mathbf{x} = [\mathbf{z}, \mathbf{z}, -\mathbf{z}] \end{aligned}$$

The ordering is a semantic that determines \mathbf{y} and computing it requires comparing coordinates: $\mathbf{y} = 1$ if $\mathbf{x}_2\mathbf{x}_3 > 0$, $\mathbf{y} = 2$ if $\mathbf{x}_1\mathbf{x}_3 > 0$, and $\mathbf{y} = 3$ otherwise. In words, the semantic feature is global. However, $\mathbf{z} = \mathbf{x}_1 + \mathbf{x}_2 + \mathbf{x}_3$, which means that \mathbf{z} is determined regardless of where the negative sign is, i.e. it is not global. Here, a random permutation $T(\mathbf{x}, \delta)$ of the coordinates in \mathbf{x} is a semantic corruption: as $T(\mathbf{x}, \delta)$ permutes the location of the negation, $T(\mathbf{x}) \mid \mathbf{y}, \mathbf{z}$ is distributed identically to $T(\mathbf{x}) \mid \mathbf{z}$. We give corruptions for global semantics in vision and language tasks, that retain non-global features.

Patch randomization. Object recognition tasks where the object is a shape that can satisfy the global property. For illustration, consider differentiating cows and penguins in natural images; here, shape is a global semantic feature that structure multiple patches. Permuting patches via **patch randomization** (PATCH-RAND), like in fig. 1a, corrupts global semantics.

N-gram randomization. Tasks like natural language inference (NLI) — where the goal is determining if a premise sentence entails a hypothesis — satisfy the global-semantics property. Consider this example: the sentence "Bob speaks but Jon does not" contradicts "Jon speaks but Bob does not" but entails "Bob speaks". The meaning is inferred from a global structure on the words and the order they appear in. Here, randomizing the order of the words corrupts the semantics: For example, one randomized order of the sentence "Jon speaks but Bob does not" is "Bob speaks but Jon does not"; the former entails "Jon speaks" but the latter contradicts it. We randomize the order by permuting different n -grams in each sentence; we call this **n-gram randomization** (NGRAM-RAND).

3.2 Semantic corruptions via masking

The second corruption we build focuses on cases where certain subsets of the covariates are necessary part of semantics. Masking, by removing that subset or setting it to a constant, corrupts semantics. Formally, we corrupt the semantics by replacing subsets \mathbf{x}_S with a value that is out of support: for example, in images where pixels lie in $(0, 1)$, we corrupt $\mathbf{x} = [\mathbf{x}_S, \mathbf{x}_{-S}]$ as $\mathbf{x}_{\text{corrupted}} = [0 * \mathbf{x}_S, \mathbf{x}_{-S}]$.

As an illustrative example, consider a family $\mathcal{F} = \{p_D\}_{D \in \mathbb{R}}$ with varying nuisance-label relationships. With \mathbf{a}, \mathbf{b} being random uniform binary random variables, $\mathbf{e}(\rho)$ as the exponential distribution with parameter ρ , and $s_+(u) = \log(1 + \exp(u))$ as softplus, let sampling from $p_D(\mathbf{y}, \mathbf{z}, \mathbf{x})$ be:

$$\mathbf{y} = \mathbf{a} \oplus \mathbf{b}, \mathbf{z} \sim \mathbf{e}(s_+(D * (2\mathbf{y} - 1))) \quad (1)$$

$$\mathbf{x} = [(2\mathbf{a} - 1)\mathbf{z}, (2\mathbf{b} - 1)\mathbf{z}]. \quad (2)$$

For such a family, we show that masking out coordinate \mathbf{x}_1 is a semantic corruption: $T(\mathbf{x}) = [0, \mathbf{x}_2]$ satisfies $T(\mathbf{x}) \perp\!\!\!\perp \mathbf{y} \mid \mathbf{z}$ and $T(\mathbf{x}) \not\perp\!\!\!\perp \mathbf{z}$. First, due to \mathbf{y} being computed as an XOR function of \mathbf{a}, \mathbf{b} , it holds that $\mathbf{b} \perp\!\!\!\perp \mathbf{y}$. Then, due to \mathbf{z} only relying on \mathbf{y} and exogenous noise, $\mathbf{b} \perp\!\!\!\perp (\mathbf{y}, \mathbf{z})$ which implies $\mathbf{b} \perp\!\!\!\perp \mathbf{y} \mid \mathbf{z}$. Given \mathbf{z}, \mathbf{b} determines \mathbf{x}_2 , so $\mathbf{b} \perp\!\!\!\perp \mathbf{y} \mid \mathbf{z} \implies \mathbf{x}_2 \perp\!\!\!\perp \mathbf{y} \mid \mathbf{z} \implies T(\mathbf{x}) \perp\!\!\!\perp \mathbf{y} \mid \mathbf{z}$. Noting that the norm $\|T(\mathbf{x})_2\| = \mathbf{z} \implies T(\mathbf{x}) \not\perp\!\!\!\perp \mathbf{z}$.

Region-of-interest-masking for object recognition. Semantics in images can often be localized to regions-of-interest. For example, in detecting cardiomegaly, the region-of-interest is the middle of the chest where the heart resides. Masking out the region of interest removes centrally located semantic information from the chest X-ray (fig. 1b). We call this ROI-MASK.

Premise-masking for NLI. Semantic features in NLI rely on the meanings of the premise and the hypothesis sentences: for example, the premise states the occurrence of an event ("Alice sat while Bob stood.") which can entail ("Alice sat.") or contradict ("Bob sat.") the hypothesis. The information about the setup in the premise is therefore crucial to detect entailment or contradiction. If the context given by the premise is blocked out, the hypothesis sentence can predict the label only due to nuisances. Thus, masking the premise is a semantic corruption for NLI that retains features in the hypothesis; we call this PREM-MASK.

3.3 Semantic corruptions via frequency and intensity filters

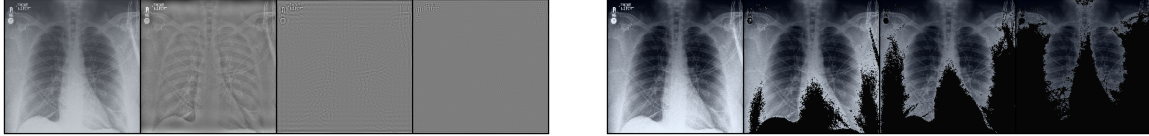
PATCH-RAND relies on differences in relative size and ROI-MASK relies on differences in spatial position. We consider two aspects of the image that are not spatial, frequency and pixel-intensity, and give corruptions for features that depend on these aspects. Semantics can appear as signals in a particular region of the frequency spectrum, or appear at a particular luminosity in the image. For example, consider detecting cardiomegaly from chest X-rays, where the heart appears as an object formed of bright pixels with little variation in intensity across the pixels; the latter suggests that the heart features are low-frequency signals.

This observation motivates corruptions along the axes of frequency and pixel-intensity: **frequency filtering (FREQ-FILTER)** and **intensity filtering (INT-FILTER)**. FREQ-FILTER zeroes-out frequencies in the discrete fourier domain, while INT-FILTER zero-out pixels based on their intensities. See fig. 2 for how FREQ-FILTER and INT-FILTER corrupt the heart region. FREQ-FILTER and INT-FILTER require characterizing semantic features in frequency and intensity spaces; this is in contrast to ROI-MASK that is based on characterizing the position in pixel space that the semantics occur in.

3.4 Using semantic corruptions in practice

For each method in table 1, we use a semantic corruption $T(\mathbf{x})$ in building a biased model $p_{tr}(\mathbf{y} \mid T(\mathbf{x}))$. For reweighting-NURD, we replace $p_{tr}(\mathbf{y} \mid \mathbf{z})$ with $p_{tr}(\mathbf{y} \mid T(\mathbf{x}))$, for DFL and POE, we replace the model $p_{tr}(\mathbf{y} \mid \mathbf{z})$ with $p_{tr}(\mathbf{y} \mid T(\mathbf{x}))$, and for JTT, we use $p_{tr}(\mathbf{y} \mid T(\mathbf{x}))$ as the identification model.

Choosing the corruption parameter. To corrupt with PATCH-RAND, NGRAM-RAND, and ROI-MASK, FREQ-FILTER, one must select a size parameter and to corrupt with INT-FILTER, one must specify an intensity threshold. For NURD, JTT, POE and DFL, we select corruption parameters with the same validation schemes



(a) Corruption via FREQ-FILTER. Original image to the left followed by zeroing out 14, 56, 112 of the lowest frequencies. The heart features are corrupted at 56.

(b) Corruption via INT-FILTER. Original image to the left followed by zeroing out pixels with intensities above the 80%, 60%, 40%. Heart features look corrupted at 40%.

Figure 2: Semantic corruptions of chest X-rays via FREQ-FILTER and INT-FILTER respectively.

used to select other hyperparameters in each respective paper. We also report results for all corruption parameters in [appendix B.2](#), showing that all semantic corruptions except INT-FILTER are not sensitive to the parameters, and lead to models that outperform ERM.

4 Experiments

In this section, we study semantic corruptions in powering NURD [7], JTT [6], and POE and DFL [4]. To be faithful to the original evaluations of each method, we run them on tasks from their respective papers: NURD on waterbirds, JTT on waterbirds and NLI where the nuisance is the presence of a negation word, and POE and DFL on NLI evaluated on a challenging test dataset, HANS [11]. Further, we run NURD on chest X-rays but focus on the task of cardiomegaly detection rather the original pneumonia detection [7] because pneumonia detection even with known-nuisances is not performant. See [appendix B](#) for implementation details.

Methods, metrics and model selection. For images, we corrupt semantics with PATCH-RAND, a central ROI-MASK, FREQ-FILTER, and INT-FILTER. For text, we corrupt semantics with NGRAM-RAND and PREM-MASK. To point to the value of *semantic* corruptions relative to existing data augmentations, we also build biased models with two baseline transformations that corrupt features: random cropping (RAND-CROP) and adding gaussian noise (GAUSS-NOISE), both common data augmentations [12]. We report the average test accuracy for every method. To be able to compare to what JTT is trained for in Liu et al. [6], we report worst-group accuracy in the test set for JTT. For each method, we compare the performance of the original method to that of the methods run with semantic corruption (including the baselines).

For every method we run with semantic corruptions, group annotations and nuisances are *unavailable* in the training data. Known-nuisance versions of POE, DFL, and NURD use direct knowledge of one or more nuisances during training. In choosing parameters and early stopping, like Liu et al. [6] do with vanilla JTT, JTT with corruptions uses validation group annotations. For selecting corruption parameters for other methods, we follow validation schemes mentioned in the respective papers: for NURD we follow Puli et al. [7] and use a validation set weighted to have independent nuisance and label, and for POE/DFL, we follow Mahabadi et al. [4] and use a validation dataset of 1000 samples from the HANS training dataset.

4.1 Object recognition tasks

To be faithful to the original evaluations of each method, we evaluate JTT on waterbirds, and NURD on both waterbirds and detecting cardiomegaly; both tasks have images of size $224 \times 224 \times 3$. For both tasks, we use PATCH-RAND (of patch sizes 7, 14, 28, 56), ROI-MASK (of mask sizes 112, 140, 168, 196), FREQ-FILTER (of high-pass filter sizes 196, 168, 140, 112), and INT-FILTER (of intensity thresholds 0.1, 0.2, 0.3, 0.4) as semantic corruptions. For the baseline RAND-CROP, we use sizes 7, 14, 28, 56 and for GAUSS-NOISE, we use variances 0.01, 0.25, 1, 4. Both Puli et al. [7] and Liu et al. [6] use the raw waterbirds data from Sagawa et al. [9], where the task is detecting the type of bird (water or land) from images where the background is a nuisance. Unlike Liu et al. [6], Puli et al. [7] process the waterbirds to get a different setup from Sagawa et al. [9]. To stay true to the original evaluations of the methods, we recreate the setups as described in their respective papers.

NURD on waterbirds. For NURD, we recreate the waterbirds experiment from Puli et al. [7] where the full waterbirds data from Sagawa et al. [9] was subsampled into training, validation, and test datasets each with label balance. However, unlike Sagawa et al. [9], the validation data comes from the same distribution as the training data. The training and validation datasets have 90% waterbirds on backgrounds with water and 90% landbirds on backgrounds with land. The test data has a flipped relationship. Known- nuisance NURD uses an additional label denoting the background-type as the nuisance.

Table 2 shows the results. Selecting the size hyperparameter based on the average accuracy over 10 seeds using NURD’s validation approach gives size 14 for PATCH-RAND (86.9%), size 196 for ROI-MASK (86.9%), size 168 for FREQ-FILTER (83.5%), and threshold 0.2 for INT-FILTER (86.9%). Consider the gap between ERM and known- nuisance NURD. NURD with PATCH-RAND, ROI-MASK, FREQ-FILTER, and INT-FILTER close 99%, 99%, 82%, 99% of the gap respectively. NURD with these semantic corruptions outperforms ERM (68.0%) and NURD with RAND-CROP (82.8%) and GAUSS-NOISE (82.0%). Additionally, in table 7 in appendix B, we give the results for all corruption parameters, showing that NURD with semantic corruptions is insensitive to hyperparameters of the corruption and outperforms ERM.

JTT on waterbirds. For JTT, we repeat the waterbirds experiment from Liu et al. [6] which uses the original data from Sagawa et al. [9]. The training data has 95% waterbirds on backgrounds with water and 95% landbirds on backgrounds with land. Both the validation and test datasets have bird label independent of the background. The groups here are subsets of the data that correspond to a pair of values of bird-type and background-type. Like vanilla JTT, we use group annotations in the validation data to compute worst-group error and early stop training when using PATCH-RAND and ROI-MASK. The results for vanilla JTT are from our run using the optimal hyperparameters from Liu et al. [6].

Table 3 shows the results. Selecting the corruption hyperparameters on the validation worst-group accuracy gives size 14 for PATCH-RAND (89%), size 196 for ROI-MASK (88.2%), size 112 for FREQ-FILTER (87.2%), and threshold 0.4 for INT-FILTER (87.0%). JTT with these semantic corruptions outperforms ERM (72.0%), vanilla JTT (86.5%), and JTT with the baseline corruptions RAND-CROP (59.2%) and GAUSS-NOISE (71.0%). Additionally, table 9 shows that JTT with PATCH-RAND and ROI-MASK outperforms JTT with the baseline corruptions and ERM at every patch/border-size.

NURD on detecting cardiomegaly In chest X-ray classification, differences between hospitals, like the scanners used to produce the X-rays, are known to correlate thoracic conditions with non-physiological aspects in the image; for example, only some scanners render the air in the lungs in white [13]. We consider the shape-based object recognition task of cardiomegaly (an irregularly sized heart) detection and, following Puli et al. [7], construct a dataset from two chest X-ray datasets: chexpert [14] and MIMIC [15]. The training and validation datasets have 90% cardiomegaly images from MIMIC and 90% healthy

Table 2: Mean and standard error of test accuracy across 10 seeds of NURD with semantic corruptions on waterbirds. *Known-z* NURD uses a label for the type of background as the nuisance. Consider the gap between ERM and known- nuisance NURD. NURD with semantic corruptions PATCH-RAND, ROI-MASK, FREQ-FILTER, and INT-FILTER close 99%, 99%, 82%, 99% of the gap respectively. NURD with semantic corruptions outperforms ERM and NURD with RAND-CROP and GAUSS-NOISE.

Method	test acc.
<i>Known-z</i> NURD	87.2 ± 1.0%
PATCH-RAND	86.9 ± 1.2%
ROI-MASK	86.9 ± 1.7%
FREQ-FILTER	83.5 ± 1.1%
INT-FILTER	86.9 ± 1.1%
RAND-CROP	82.8 ± 1.8%
GAUSS-NOISE	82.0 ± 2.6%
ERM	68.0 ± 1.9%

Table 3: Test worst-group accuracies of JTT on waterbirds. JTT with semantic corruptions outperforms ERM, vanilla JTT, and JTT with baseline corruptions (RAND-CROP and GAUSS-NOISE).

Method	test worst-group acc.
<i>Vanilla</i> JTT	86.5%
PATCH-RAND	89.0%
ROI-MASK	88.2%
FREQ-FILTER	87.2%
INT-FILTER	87.0%
RAND-CROP	59.1%
GAUSS-NOISE	71.0%
ERM	72.0%

images from chexpert, while the test data has a flipped relationship. Known-nuisance NURD uses hospital identity as the nuisance.

See [table 4](#) for results. Selecting the corruption parameters based on the mean accuracy over 10 seeds using NURD’s validation approach gives size 14 for PATCH-RAND (77%), size 196 for ROI-MASK (78.7%), size 168 for FREQ-FILTER (76.0%), and threshold 0.1 for the INT-FILTER (71.0%). Consider the gap between ERM and known-nuisance NURD. NURD with PATCH-RAND, ROI-MASK, FREQ-FILTER, and INT-FILTER close 72%, 82%, 65%, 35% of the gap respectively. NURD with all these corruptions, outperforms ERM (65.3%) and NURD with GAUSS-NOISE (69%), and all but INT-FILTER outperform NURD with RAND-CROP (75%). Additionally, we give the results for all corruption parameters in [table 7](#) in [appendix B](#); this table shows that NURD with PATCH-RAND and ROI-MASK are *insensitive to hyperparameters* and outperform ERM (65.3%).

4.2 Natural language inference (NLI)

For methods POE, DFL, and JTT, we use the MNLI dataset [16] during training. The evaluations of these methods in their respective papers have different nuisances and, consequently, different test sets. In accordance, we describe the setup and the results separately. We use NGRAM-RAND (sizes 1, 2, 3, 4) to produce nuisances for both setups.

POE and DFL For POE and DFL, we report test accuracies on the HANS dataset [11] as in Mahabadi et al. [4]. HANS was created to test the reliance of models on three known nuisances: 1) lexical overlap, 2) subsequence match, and 3) constituent matching subtrees in the parse trees. Known-nuisance POE and DFL use exact knowledge of these nuisances.

[Table 5](#) gives the mean test accuracies over 4 seeds. For both DFL and POE, selecting the size hyperparameter based on the average accuracy on a small subset of the HANS training data (1000 samples) gives $n = 3$. With this size, POE with this size achieves 66.7%, improving over POE with known nuisances (66.3%). DFL with NGRAM-RAND of size 3, achieves 68.4%, closing 84% of the gap between ERM and known-nuisance DFL (69.3%). POE and DFL with PREM-MASK (PM) close 33% and 28% of the gap between ERM and when the methods have knowledge of \mathbf{z} . We expect the methods with NGRAM-RAND do better than with PREM-MASK because the latter corrupts nuisances like lexical overlap between premise and hypothesis that HANS focuses on. Additionally, we give results for all n -gram sizes in [table 10](#) in [appendix B](#), showing that POE and DFL beat ERM for all n -gram sizes.

JTT For JTT, we repeat the NLI experiment from Liu et al. [6], where the presence of a negation word in the hypothesis sentence is the nuisance. The groups here are subsets of the data that correspond to a value of the label and whether or not there is a negation word in the hypothesis. Vanilla JTT uses group annotations in the validation data to tune the hyperparameters and early stop training. For each n -gram size, we run JTT with NGRAM-RAND for two values of the

Table 4: Mean and standard error of test accuracy across 10 seeds of NURD on chest X-rays. *Known-nuisance* NURD uses the hospital as the nuisance. Consider the gap between ERM and known-nuisance NURD. NURD with PATCH-RAND, ROI-MASK, FREQ-FILTER, and INT-FILTER close 72%, 82%, 65%, 35% of the gap respectively. Except with INT-FILTER, NURD with semantic corruptions outperforms ERM and NURD with baseline corruptions.

Method	test acc.
<i>Known-z</i> NURD	$81.7 \pm 0.3\%$
PATCH-RAND	$77.0 \pm 1.2\%$
ROI-MASK	$78.7 \pm 0.3\%$
FREQ-FILTER	$76.0 \pm 0.6\%$
INT-FILTER	$71.0 \pm 1.0\%$
RAND-CROP	$75.0 \pm 0.7\%$
GAUSS-NOISE	$69.0 \pm 1.9\%$
ERM	$65.3 \pm 1.1\%$

Table 5: Mean and standard deviation of accuracies (over 4 seeds) on the HANS dataset. The results for POE and DFL that use known nuisances are given under *known*. POE with NGRAM-RAND (NR) performs better than known-nuisance POE. DFL with (NR) closes 84% of the gap between ERM and known-nuisance DFL. POE and DFL with PREM-MASK (PM) close 33% and 28% of the gap between ERM and the respective method with known \mathbf{z} .

Method	HANS test accuracy
POE, <i>known-z</i>	$66.3 \pm 0.6\%$
POE, NR	$66.7 \pm 1.5\%$
POE, PM	$64.5 \pm 1.9\%$
DFL, <i>known-z</i>	$69.3 \pm 0.2\%$
DFL, NR	$68.4 \pm 1.5\%$
DFL, PM	$65.2 \pm 0.7\%$
ERM	$63.6 \pm 1.1\%$

number of epochs of training for the identification model: 2, 3. Following the hyperparameter selection procedure from Liu et al. [6], for each n -gram size, we give the results for the run with the higher validation worst-group accuracy. We run *vanilla* JTT using the reported optimization hyperparameters from [6].

Table 6 gives the results. Selecting the size hyperparameter for NGRAM-RAND using validation worst-group accuracy, like Liu et al. [6] do for JTT, gives $n = 1$ with test worst-group accuracy of 74.3%, better than vanilla JTT’s 71.3%. Additionally, table 11 shows that JTT using NGRAM-RAND at *every* size or PREM-MASK perform better than both vanilla JTT (71.3%) and ERM (67.9%).

5 Related work

Spurious-correlation avoiding methods (SCAMs) like [5, 7, 8, 17, 18] assume the nuisance is available as additional knowledge during training. Semantic corruptions offer a complementary approach to hand-crafting nuisances or obtaining auxiliary labels, by capturing every nuisance that remains after corruption (e.g. non-global nuisances remain after PATCH-RAND).

Two-model SCAMs like Learning from Failure (LFF) [19] and JTT [6] assume they can build a biased model that exploits the nuisance and use it to reduce a second model’s dependence on the nuisance. Both methods train the second model with weighted cross-entropy where higher weights are assigned to samples misclassified by the biased model. While LFF jointly trains both models and uses generalized cross entropy [20] for the biased model, JTT builds them in subsequent stages and uses cross-entropy to build the biased model. When the biased model relies on semantics, upweighting misclassified samples produces data with a different label-semantic relationship from the one in the training data. Models trained on such data are suboptimal on test data with the same semantic relationship as the training data. Using semantic corruptions reduces the identification model’s reliance on the semantics, as evidenced by JTT with semantic corruptions improving over vanilla JTT. We do not run LFF as vanilla JTT outperforms it.

Sinha et al. [21] use techniques like PATCH-RAND to restrict supports in self-supervised learning and generative modeling. Carlucci et al. [22] use PATCH-RAND images to encourage a model to recover semantic structure. In contrast, we use PATCH-RAND to corrupt semantics and build biased models that rely on the nuisances, which help build predictive models that avoid reliance on nuisances. Work like [7, 8] also use semantic corruptions without pointing out the reliance on knowledge about semantic features in producing nuisances. He et al. [8] use the hypothesis as a nuisance to build a biased model for NLI; this is the masking based semantic corruption PREM-MASK. Puli et al. [7] focus on chest X-ray classification, and use the out-of-body border of the X-ray as a nuisance; this is corrupting semantics via ROI-MASK.

Work like Bahng et al. [23] uses CNNs with small receptive fields (RFs), to help capture non-global nuisances. However, their method is typically limited to very small filters because at size 3x3, deep neural networks like VGG detect global semantics like shapes. In contrast, the size choice in PATCH-RAND has no bearing on the choice of the model; we used default vision models. Bras et al. [24] automatically identify and remove examples with nuisances using adversarial filtering, but risk removing genuinely easy examples. Qin et al. [25] work solely with vision transformers and point out that nuisances are the only reason labels can be predicted from transformations akin to patch-randomized images. They propose to encourage transformers to have predictions and representations of the original images be dissimilar from those of patch-randomized ones. In contrast, our work applies to general flexible models and shows that semantic corruptions can be used to break the label’s relationship with nuisances in the original images.

6 Discussion

We study the use of semantic knowledge in building robust models. Given a procedure to corrupt semantics, anything that predicts the label in the corrupted input is a nuisance. Using semantic corruptions,

Table 6: Worst-group and average test accuracies of JTT on NLI. JTT with PREM-MASK (PM) and NGRAM-RAND (NR) outperforms vanilla JTT and ERM.

	Worst-group	Avg.
<i>Vanilla</i> JTT	71.3%	79.1%
JTT + PM	72.1%	79.9%
JTT + NR	74.3%	79.7%
ERM	67.9%	82.4%

practitioners can run different kinds of spurious-correlation avoiding methods (SCAMS) (NURD, JTT, DFL, POE). With these semantic corruptions, methods like NURD and DFL perform close to how they would with known nuisances, and methods like JTT perform better than how they would when assuming ERM on the raw covariates yields the nuisance.

Limitations. The quality of any semantic corruption, and thus the quality of the results, depends on the extent to which semantics are destroyed and nuisances are retained. PATCH-RAND and NGRAM-RAND are built to corrupt global semantics, ROI-MASK to corrupt semantics in the region-of-interest (ROI), and PREM-MASK to corrupt the semantic context in the premise. When applied blindly, these methods may retain semantics or corrupt nuisances.

For example, when PATCH-RAND is used blindly on covariates with non-global semantics, the biased model may rely on said semantics; this in turn guides the predictive model to ignore these semantics and, thus, lose predictive performance. Alternatively, when nuisances are global, PATCH-RAND may corrupt them. For example in detecting cows and penguins, other nuisance animals (like dogs) may co-occur with cows more often; PATCH-RAND would corrupt this nuisance animal. Using PATCH-RAND in a SCAM for such tasks could lead to non-robust predictive models that rely on corrupted nuisances.

However, our experiments show blind usage does not always lead to poor performance despite some nuisances having similar properties to the semantics that are being corrupted. In both classifying waterbirds and NLI, there exist non-global semantics, like small beaks and individual words, that are not corrupted by PATCH-RAND and NGRAM-RAND respectively. However, in our Waterbirds and NLI experiments, we show models built using semantic corruptions close more than 80% of the gap in test performance between ERM and the methods that use known nuisances.

Summary. Semantic corruptions power SCAMS to build models robust to spurious correlations without requiring extra annotations in the form of known nuisances during training or relying on hard to verify assumptions like ERM-trained models relying on nuisances. As discussed above, our experiments show that using semantic corruptions in SCAMS leads to models more robust than ERM and JTT even when the corruptions may have corrupted some nuisances. These two properties demonstrate the value of semantic corruptions as a way to build robust models.

Acknowledgements

The authors were supported by NIH/NHLBI Award R01HL148248, NSF Award 1922658 NRT-HDR: FUTURE Foundations, Translation, and Responsibility for Data Science, NSF CAREER Award 2145542, and Samsung Advanced Institute of Technology (Next Generation Deep Learning: From Pattern Recognition to AD). Aahlad Puli is supported by the Apple Scholars in AI/ML PhD fellowship. Nitish Joshi is supported by the NSF Graduate Research Fellowship grant number 1839302.

References

- [1] Sara Beery, Grant Van Horn, and Pietro Perona. Recognition in terra incognita. In *Proceedings of the European conference on computer vision (ECCV)*, pages 456–473, 2018.
- [2] Martin Arjovsky, Léon Bottou, Ishaan Gulrajani, and David Lopez-Paz. Invariant risk minimization. *arXiv preprint arXiv:1907.02893*, 2019.
- [3] Robert Geirhos, Jörn-Henrik Jacobsen, Claudio Michaelis, Richard Zemel, Wieland Brendel, Matthias Bethge, and Felix A. Wichmann. Shortcut learning in deep neural networks, 2020.
- [4] Rabeeh Karimi Mahabadi, Yonatan Belinkov, and James Henderson. End-to-end bias mitigation by modelling biases in corpora. *arXiv preprint arXiv:1909.06321*, 2019.
- [5] Maggie Makar, Ben Packer, Dan Moldovan, Davis Blalock, Yoni Halpern, and Alexander D’Amour. Causally-motivated shortcut removal using auxiliary labels. In *AISTATS*, 2022.

- [6] Evan Z Liu, Behzad Haghgoo, Annie S Chen, Aditi Raghunathan, Pang Wei Koh, Shiori Sagawa, Percy Liang, and Chelsea Finn. Just train twice: Improving group robustness without training group information. In *International Conference on Machine Learning*, pages 6781–6792. PMLR, 2021.
- [7] Aahlad Manas Puli, Lily H Zhang, Eric Karl Oermann, and Rajesh Ranganath. Out-of-distribution generalization in the presence of nuisance-induced spurious correlations. In *International Conference on Learning Representations*, 2022. URL <https://openreview.net/forum?id=12RoR2o32T>.
- [8] He He, Sheng Zha, and Haohan Wang. Unlearn dataset bias in natural language inference by fitting the residual. *arXiv preprint arXiv:1908.10763*, 2019.
- [9] Shiori Sagawa, Pang Wei Koh, Tatsunori B Hashimoto, and Percy Liang. Distributionally robust neural networks for group shifts: On the importance of regularization for worst-case generalization. *arXiv preprint arXiv:1911.08731*, 2019.
- [10] Jacob Devlin, Ming-Wei Chang, Kenton Lee, and Kristina Toutanova. Bert: Pre-training of deep bidirectional transformers for language understanding. In *NAACL*, 2019.
- [11] R Thomas McCoy, Ellie Pavlick, and Tal Linzen. Right for the wrong reasons: Diagnosing syntactic heuristics in natural language inference. *arXiv preprint arXiv:1902.01007*, 2019.
- [12] Connor Shorten and Taghi M Khoshgoftaar. A survey on image data augmentation for deep learning. *Journal of big data*, 6(1):1–48, 2019.
- [13] John R Zech, Marcus A Badgeley, Manway Liu, Anthony B Costa, Joseph J Titano, and Eric Karl Oermann. Variable generalization performance of a deep learning model to detect pneumonia in chest radiographs: a cross-sectional study. *PLoS medicine*, 15(11):e1002683, 2018.
- [14] Jeremy Irvin, Pranav Rajpurkar, Michael Ko, Yifan Yu, Silvana Ciurea-Ilcus, Chris Chute, Henrik Marklund, Behzad Haghgoo, Robyn Ball, Katie Shpanskaya, et al. Chexpert: A large chest radiograph dataset with uncertainty labels and expert comparison. In *Proceedings of the AAAI Conference on Artificial Intelligence*, volume 33, pages 590–597, 2019.
- [15] Alistair EW Johnson, Tom J Pollard, Nathaniel R Greenbaum, Matthew P Lungren, Chih-ying Deng, Yifan Peng, Zhiyong Lu, Roger G Mark, Seth J Berkowitz, and Steven Horng. Mimic-cxr-jpg, a large publicly available database of labeled chest radiographs. *arXiv preprint arXiv:1901.07042*, 2019.
- [16] Adina Williams, Nikita Nangia, and Samuel Bowman. A broad-coverage challenge corpus for sentence understanding through inference. In *Proceedings of the 2018 Conference of the North American Chapter of the Association for Computational Linguistics: Human Language Technologies, Volume 1 (Long Papers)*, pages 1112–1122. Association for Computational Linguistics, 2018. URL <http://aclweb.org/anthology/N18-1101>.
- [17] Victor Veitch, Alexander D’Amour, Steve Yadlowsky, and Jacob Eisenstein. Counterfactual invariance to spurious correlations: Why and how to pass stress tests. *arXiv preprint arXiv:2106.00545*, 2021.
- [18] Christopher Clark, Mark Yatskar, and Luke Zettlemoyer. Don’t take the easy way out: Ensemble based methods for avoiding known dataset biases. *arXiv preprint arXiv:1909.03683*, 2019.
- [19] Junhyun Nam, Hyuntak Cha, Sungsoo Ahn, Jaeho Lee, and Jinwoo Shin. Learning from failure: De-biasing classifier from biased classifier. *Advances in Neural Information Processing Systems*, 33: 20673–20684, 2020.
- [20] Zhilu Zhang and Mert Sabuncu. Generalized cross entropy loss for training deep neural networks with noisy labels. *Advances in neural information processing systems*, 31, 2018.
- [21] Abhishek Sinha, Kumar Ayush, Jiaming Song, Burak Uzkent, Hongxia Jin, and Stefano Ermon. Negative data augmentation. *arXiv preprint arXiv:2102.05113*, 2021.

- [22] Fabio M Carlucci, Antonio D’Innocente, Silvia Bucci, Barbara Caputo, and Tatiana Tommasi. Domain generalization by solving jigsaw puzzles. In *Proceedings of the IEEE/CVF Conference on Computer Vision and Pattern Recognition*, pages 2229–2238, 2019.
- [23] Hyojin Bahng, Sanghyuk Chun, Sangdoon Yun, Jaegul Choo, and Seong Joon Oh. Learning de-biased representations with biased representations. In *International Conference on Machine Learning*, pages 528–539. PMLR, 2020.
- [24] Ronan Le Bras, Swabha Swayamdipta, Chandra Bhagavatula, Rowan Zellers, Matthew E. Peters, Ashish Sabharwal, and Yejin Choi. Adversarial filters of dataset biases. In *ICML*, 2020.
- [25] Yao Qin, Chiyuan Zhang, Ting Chen, Balaji Lakshminarayanan, Alex Beutel, and Xuezhi Wang. Understanding and improving robustness of vision transformers through patch-based negative augmentation. *arXiv preprint arXiv:2110.07858*, 2021.

A Further details about spurious-correlation avoiding methods

NURD. Focusing on mitigating spurious correlations, Puli et al. [7] identify a conditional that has performance guarantees on every test distribution within a family of distributions with varying nuisance-label relationships: $p_{te} \in \mathcal{F}$. They develop NURD to learn the conditional using data only from $p_{tr} \neq p_{te}$. NURD uses 1) the *nuisance-randomized distribution*, $p_{\perp}(\mathbf{y}, \mathbf{z}, \mathbf{x}) = p(\mathbf{y})p_{\perp}(\mathbf{z})p(\mathbf{x} | \mathbf{y}, \mathbf{z})$, where $\mathbf{z} \perp_{p_{\perp}} \mathbf{y}$, and 2) an *uncorrelating representation* $r(\mathbf{x})$ for which $\mathbf{z} \perp_{p_{\perp}} \mathbf{y} | r(\mathbf{x})$. NURD builds models of the form $p_{\perp}(\mathbf{y} | r(\mathbf{x}))$ using $r(\mathbf{x})$ that are most informative of the label.

We run reweighting-NURD, which uses a biased model $p_{tr}(\mathbf{y} | \mathbf{z})$ as an importance weight to compute loss under the nuisance-randomized distribution: $p_{\perp}(\mathbf{y}, \mathbf{z}, \mathbf{x}) = \frac{p_{tr}(\mathbf{y})}{p_{tr}(\mathbf{y} | \mathbf{z})} p_{tr}(\mathbf{y}, \mathbf{z}, \mathbf{x})$.

To run reweighting-NURD with semantic corruptions, we replace $p_{tr}(\mathbf{y} | \mathbf{z})$ with $p_{tr}(\mathbf{y} | T(\mathbf{x}))$ for a semantic corruption $T(\mathbf{x})$. Semantic corruptions are noisy functions of \mathbf{x} : with noise ϵ such that $(\mathbf{y}, \mathbf{z}, \mathbf{x}) \perp_{p_D} \epsilon$, $T(\mathbf{x}) = U(\mathbf{x}, \epsilon)$. This implies

$$\mathbf{y} \perp_{p_{\perp}} \epsilon | \mathbf{x} \implies \mathbf{y} \perp_{p_{\perp}} \mathbf{x}, \epsilon | \mathbf{x} \implies \mathbf{y} \perp_{p_{\perp}} T(\mathbf{x}) | \mathbf{x}$$

Thus, $r(\mathbf{x}) = \mathbf{x}$ is uncorrelating and $p_{\perp}(\mathbf{y} | \mathbf{x})$ achieves the optimality guarantees in Puli et al. [7]. These optimality guarantees imply that regardless of the test nuisance-label relationship, $p_{\perp}(\mathbf{y} | \mathbf{x})$ will achieve optimal performance within the class of models like $p_{\perp}(\mathbf{y} | r(\mathbf{x}))$.

End-to-end bias mitigation. Mahabadi et al. [4] consider two methods to train a *biased* model $p_{tr}(\mathbf{y} | \mathbf{z})$ and a base predictive model jointly to make the base model predict without relying on the biases. The methods use and fine-tune a BERT model [10] and do not propagate the gradients of the biased model to update the common parameters (token embeddings in this case). They propose 1) POE, where the log of the product of the predictions (the output probabilities) of the two models is used to compute the classification loss and 2) DFL, where the biased model is used to weight the cross-entropy loss for the base model.

The intuition for POE is that the samples for which the biased model classifies correctly will not contribute to the gradients of the base model; thus the base model focuses more on classifying samples that the biased model misclassifies. The DFL algorithm weights each sample as the biased model’s predicted probability of all but the label, exponentiated with $\gamma > 0$. This downweights samples that the biased model classifies correctly which in turn mitigates the base model’s reliance on a nuisance which only helps predict the downweighted samples correctly.

Mahabadi et al. [4] build the biased model as $p_{tr}(\mathbf{y} | \mathbf{z})$ with known nuisances \mathbf{z} . We replace this model with $p_{tr}(\mathbf{y} | T(\mathbf{x}))$ for a semantic corruption $T(\mathbf{x})$.

Just Train Twice (JTT). JTT works in two stages: 1) build an "identification" model via ERM on the training data to isolate samples that are misclassified due to reliance on the nuisances and 2) train a model via ERM on data with the loss for the misclassified samples upweighted (by constant λ). The identification model in JTT is built to be a biased model. When the identification model equals $p_{tr}(\mathbf{y} | \mathbf{z})$, it exactly misclassifies the samples in the groups in the minority group¹. Upweighting these samples produces a dataset with lesser dependence between the nuisance and the label. Models learned on the upweighted data depend more on the semantics.

In this work, we build the identification model on semantic corruptions i.e. we learn $p_{tr}(\mathbf{y} | T(\mathbf{x}))$. The training samples to be upweighted are the ones misclassified when predicting with the identification model on semantic-corrupted versions of the sample, i.e. $T(\mathbf{x})$. The second stage is run as in [6] with training data.

¹The minority group is the set of samples that the nuisance misclassifies. For example, when $p_{tr}(\mathbf{y} = \mathbf{z}) > p_{tr}(\mathbf{y} \neq \mathbf{z})$, then the minority group is the set of samples with $\mathbf{y} \neq \mathbf{z}$ because using only the nuisance feature results in predicting $\mathbf{y} = \mathbf{z}$.

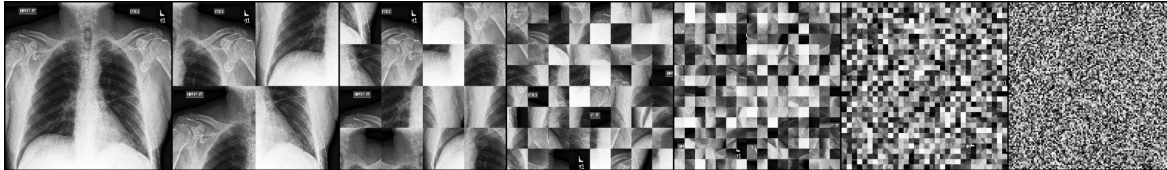


Figure 3: Example of PATCH-RAND of a chest X-ray image. The image is followed by PATCH-RANDs of size 112, 56, 28, 14, 7, 2.

B Further experimental details

B.1 Implementation details

Each experiment in the paper was run on up to 2 RTX8000 GPUs. The hyperparameters for methods which use known nuisances in the training data like NURD, POE, DFL are tuned on validation data from the training distribution. We do the same when using semantic corruptions.

Experimental details for Waterbirds For the NURD setup, the training, validation, and test datasets have 3020, 756, 800 samples respectively. We use a single architecture to parameterize the predictive model and the weight model in this experiment: two fully connected layers on top of a ResNet18 initialized at weights pretrained on Imagenet. We use the same training procedure for NURD with known nuisances or with semantic corruptions. Both models are trained with cross-entropy. The weight model is optimized with the default Adam optimizer for 20 epochs with a batch size of 64. The predictive model is optimized with the Adam optimizer for 20 epochs with a learning rate of 0.0002, a weight decay of 0.01, and a batch size of 250.

For the JTT setup, the training, validation, and test datasets have 4795, 1199, 5794 samples respectively. For JTT, we use the same model and model parameters as Liu et al. [6] using their released code. We repeat the details here for completeness. The model for both stages of JTT is a ResNet-50. Both models are optimized by stochastic gradient descent (SGD) with momentum 0.9, weight decay 1.0, and learning rate 1×10^{-5} . Both models are trained for 300 epochs with batch size 64, using batch normalization and no data augmentation. The identification model used to select samples to upweight corresponds to epoch 60 and the upweighting constant is $\lambda = 100$.

Experimental details for cardiomegaly detection. The training, validation, and test datasets are fixed across seeds and have 18000, 2000, 1000 samples respectively. To run reweighting-NURD, we use a single architecture to parameterize the predictive model and the weight model in this experiment: two fully connected layers on top of a ResNet18 initialized at weights pretrained on Imagenet. In known-nuisance NURD with the hospital as the nuisance, the biased model is an estimate of $p_{tr}(\mathbf{y} \mid \text{hospital})$, which is obtained by binning the samples based on the hospital and averaging the labels. We use the same training procedure for NURD with known nuisances or with semantic corruptions. Both weight and predictive models are trained with cross-entropy. The weight model and the predictive model are optimized with the Adam optimizer over 25 epochs with a batch size of 256, and learning rate 0.001.

Implementation details for NLI For POE and DFL, we build classifiers by fine-tuning a pretrained BERT model [10] on the data. We follow the same training procedure and hyperparameter details as used in Mahabadi et al. [4] — models were trained on the MNLI training dataset which consists of 392k examples, with a learning rate of 2×10^{-5} with a batch size of 8 using the Adam Optimizer. All models are trained for 3 epochs. The development set contains 9815 examples and the HANS test contains 30000 examples. Since the HANS dataset has only two labels — ‘entailment’ and ‘non-entailment’ — we combine the neutral and contradiction classes during inference on HANS.

For the JTT setup, Liu et al. [6] mix the training and development sets from MNLI and create their own training, validation, and test sets of sizes 206175, 82462, 123712 respectively. For JTT, we use the same

Table 7: Mean and standard error of test accuracy across 10 seeds of NURD on classifying waterbirds. *Known*-nuisance NURD uses a label for the type of background as the nuisance. Selecting the size hyperparameter based on the average accuracy over 10 seeds on the validation dataset gives 14 for PATCH-RAND, 196 for ROI-MASK, 168 for FREQ-FILTER, and 0.2 for INT-FILTER. Consider the gap between ERM and known-*nuisance* NURD. NURD with PATCH-RAND, ROI-MASK, FREQ-FILTER, and INT-FILTER close 99%, 99%, 82%, 99% of the gap respectively. NURD with these semantic corruptions outperforms ERM and NURD with RAND-CROP and GAUSS-NOISE. NURD with all semantic corruptions outperforms ERM (69.2%).

	<i>known</i> <i>z</i>	RM 196	RM 168	RM 140	RM 112	PR 7	PR 14	PR 28	PR 56	ERM
Mean	87.2%	86.9%	86.6%	86.2%	86.3%	85.6%	86.9%	82.5%	84.9%	68.0%
Std. err.	1.0%	1.1%	1.2%	1.8%	1.6%	1.4%	1.2%	2.0%	1.4%	1.9%
		FF 196	FF 168	FF 140	FF 112	IF 0.1	IF 0.2	IF 0.3	IF 0.4	
Mean		83.8%	83.5%	81.0%	80.3%	81.2%	86.9%	85.0%	81.9%	
Std. err.		1.2%	1.1%	1.4%	1.7%	1.7%	1.1%	1.5%	1.7%	
		CROP 56	CROP 28	CROP 14	CROP 7	GAUSS 0.01	GAUSS 0.25	GAUSS 1	GAUSS 4	
Mean		81.9%	80.3%	74.9%	67.9%	75.8%	74.1%	78.0%	83.9%	
Std. err.		1.5%	1.3%	1.5%	2.9%	3.2%	3.1%	3.4%	1.4%	

model and model parameters as Liu et al. [6] using their released code. We use the optimal hyperparameters reported in [6] for the learning rate, weight decay, and the upweighting constant. We repeat the details here for completeness. The model for both stages of JTT is a pretrained BERT model that is finetuned during training. Both models are optimized by the AdamW optimizer with clipping for the predictive model, no weight decay, and an initial learning rate of 2×10^{-5} . Both models are trained for 5 epochs with batch size 32 and dropout. The identification model used to select samples to upweight corresponds to epoch 2 for vanilla JTT (reported optimal in Liu et al. [6]); for JTT with semantic corruption, we select one from 2, 3 using validation group annotations. For both, the upweighting constant is $\lambda = 6$. Our runs with these parameters did not yield the test worst-group accuracy reported in [6] (72.6%); our experiments yielded a test worst-group accuracy 71.3%. We expect this may be due to the differences in the random seed; JTT is sensitive to hyperparameters and differences in order of batches may result in drops in performance.

In NGRAM-RAND, when the number of words in the sentence is not a multiple of n , there will be one k -gram ($k < n$). In implementing NGRAM-RAND, we ensure that the position of this k -gram is randomized i.e. we make sure that it does not always occur at the end of the sentence, for example. NGRAM-RAND is implemented before word-piece tokenization (which BERT uses), to ensure that we randomize words instead of subwords.

We also create a small HANS-like development set, which is used to tune the size parameter. This set is constructed by randomly sampling 1000 examples from the HANS training set, which has zero overlap with the HANS test set.

B.2 Full results tables

We give the results for all size parameters; see [table 7](#), [table 8](#), [table 9](#), [table 11](#), and [table 10](#). To report the same metrics as in [4] for POE and DFL and [7] for NURD, we report standard error for NURD and standard deviation for POE and DFL .

Table 8: Mean and standard error of test accuracy across 10 seeds of NURD on detecting cardiomegaly from chest X-rays. *Known*-nuisance NURD uses the hospital as the nuisance. Selecting the corruption parameters based on the mean accuracy over 10 seeds on the validation dataset gives 14 for PATCH-RAND, 196 for ROI-MASK, 168 for FREQ-FILTER, and 0.1 for the INT-FILTER. Consider the gap between ERM and known-nuisance NURD. NURD with PATCH-RAND, ROI-MASK, FREQ-FILTER, and INT-FILTER close 72%, 82%, 65%, 35% of the gap respectively. NURD with PATCH-RAND, ROI-MASK, FREQ-FILTER outperforms ERM and NURD with RAND-CROP and GAUSS-NOISE. NURD with PATCH-RAND and ROI-MASK outperforms ERM for all size parameters.

	<i>known</i> <i>z</i>	RM 196	RM 168	RM 140	RM 112	PR 7	PR 14	PR 28	PR 56	ERM
Mean	81.7%	78.7%	78.3%	77.2%	73.6%	76.2%	77.0%	74.9%	74.3%	65.3%
Std. err.	0.3%	0.3%	0.8%	0.8%	0.7%	1.2%	1.2%	1.0%	1.4%	1.1%

		FF 196	FF 168	FF 140	FF 112	IF 0.1	IF 0.2	IF 0.3	IF 0.4
Mean		74.4%	76.0%	75.3%	71.3%	71.0%	68.0%	62.0%	57.1%
Std. err.		1.5%	0.6%	0.9%	1.6%	1.0%	1.6%	1.8%	3.2%

		CROP 56	CROP 28	CROP 14	CROP 7	GAUSS 0.01	GAUSS 0.25	GAUSS 1	GAUSS 4
Mean		75.0%	71.4%	70.7%	67.9%	62.3%	63.5%	68.0%	69.0%
Std. err.		0.7%	1.2%	0.9%	2.3%	3.7%	3.4%	1.1%	1.9%

Table 9: Test worst-group accuracies of JTT with semantic corruptions on waterbirds. Selecting the corruption hyperparameters on the validation worst-group accuracy gives size 14 for PATCH-RAND, size 196 for ROI-MASK, size 112 for FREQ-FILTER, and threshold 0.4 for INT-FILTER. JTT with these semantic corruptions outperforms ERM, vanilla JTT, and JTT with the baseline corruptions RAND-CROP and GAUSS-NOISE. JTT with PATCH-RAND and ROI-MASK always outperforms JTT with the baseline corruptions and ERM.

<i>Vanilla</i> JTT	RM 196	RM 168	RM 140	RM 112	PR 7	PR 14	PR 28	PR 56	ERM
86.5%	88.2%	88.0%	86.9%	86.2%	89.3%	89.0%	88.9%	89.1%	72%

		FF 196	FF 168	FF 140	FF 112	IF 0.1	IF 0.2	IF 0.3	IF 0.4
		82.5%	84.5%	85.2%	87.2%	69.1%	80.0%	81.7%	87.0%

		CROP 56	CROP 28	CROP 14	CROP 7	GAUSS 0.01	GAUSS 0.25	GAUSS 1	GAUSS 4
		59.1%	0.0%	0.0%	0.0%	0.0%	0.0%	71.0%	0.0%

Table 10: Average accuracies and standard deviation over 4 seeds of POE and DFL with semantic corruptions on the HANS dataset. The results for *known* POE and DFL from [4], where both methods use known nuisances. For both methods, selecting the size hyperparameter based on the average accuracy on a small dataset (1000 samples) from the HANS training data gives $n = 3$. With this size, POE with NGRAM-RAND performs better than known-nuisance POE while DFL with NGRAM-RAND closes 84% of the gap between ERM and known-nuisance DFL .

z	POE	DFL
<i>Known</i>	66.3 ± 0.6%	69.3 ± 0.2%
1-gram	65.7 ± 2.0%	66.5 ± 1.5%
2-gram	66.0 ± 0.9%	68.5 ± 0.7%
3-gram	66.7 ± 1.5%	68.4 ± 1.5%
4-gram	66.2 ± 2.9%	65.0 ± 2.0%
ERM	—	63.6%.

Table 11: Worst-group and average test accuracies of JTT with semantic corruptions on NLI. JTT with PREM-MASK and NGRAM-RAND of every size outperforms vanilla JTT. Selecting the size hyperparameter for NGRAM-RAND using validation worst-group accuracy, like Liu et al. [6] do for vanilla JTT, gives $n = 1$. At this size, JTT with NGRAM-RAND outperforms vanilla JTT by 3% accuracy.

	Worst-group	Average
<i>Vanilla JTT</i>	71.3%	79.1%
PREM-MASK	72.1%	79.9%
1-gram	74.3%	79.7%
2-gram	71.9%	80.0%
3-gram	72.0%	80.1%
4-gram	73.4%	80.4%
ERM	67.9%	—